C. R. Physique 11 (2010) 355–361

Contents lists available at ScienceDirect

Comptes Rendus Physique

www.sciencedirect.com

Optical properties of nanotubes / Propriétés optiques des nanotubes

Carbon nanotube electromechanical resonator for ultrasensitive mass/force sensing

Résonateurs électromécaniques à nanotube de carbone, des détecteurs de masse/force ultrasensibles

Benjamin Lassagne [a,*], Adrian Bachtold [b]

[a] *Université de Toulouse, Laboratoire de Physique et de Chimie des Nano-Objets (LPCNO CNRS-INSA-UPS), UMR 5215, 31077 Toulouse cedex 4, France*
[b] *Centre d'Investigacio en Nanociencia i Nanotechnologia (CIN2), Barcelona, Spain*

ARTICLE INFO

Article history:
Available online 7 August 2010

Keywords:
Carbon nanotube
Nanoelectromechanical systems
Mixing technique
Nanofabrication
Ultrasensitive mass sensing
Coulomb blockade

Mots-clés :
Nanotube de carbone
Nano systèmes électromécaniques
Technique de mixage
Nanofabrication
Détection de masse ultrasensible
Blocage de coulomb

ABSTRACT

Controlling the mechanical motion of objects which have at least one dimension in the range of few nanometers has recently opened new avenues for fundamental science and technological developments. Carbon nanotubes are one of the most promising and suitable nano-objects for such an experimental issue. Indeed, they are an uni-dimensional system with a diameter around 1 nm, they combine exceptional mechanical and electronic properties and they are easy to manipulate and to address. We review here the basic principles of fabrication, of electromechanical actuation and detection of the nanotube motion and we present the first experimental results obtained which have allowed us to (i) understand the effect of the electromechanical on the mechanical properties; and (ii) to test the carbon nanotube capabilities for mass sensing.

RÉSUMÉ

La possibilité de contrôler le mouvement mécanique d'un objet ayant au moins une dimension de l'ordre de quelques nanomètres a récemment ouvert de nouvelles opportunités en physique fondamentale, ainsi que de développements technologiques. Les nanotubes de carbone sont l'un des nanomatériaux les plus prometteurs et les plus adaptés pour répondre à une telle problématique expérimentale. En effet ils sont uni dimensionnelles avec un diamètre de l'orde du nanomètre, ils combinent des propriétés mécaniques et électroniques exceptionnelles et ils sont faciles à manipuler et adresser. Nous présentons ici les principes de base de la fabrication, de l'actionnement électromécanique et de la détection du mouvement d'un nanotube et nous présentons les premiers résultats expérimentaux obtenus ayant permis (i) de comprendre l'influence du couplage électromécanique sur les propriétés mécaniques et, (ii) de tester les capacités des nanotubes de carbone comme détecteur de masse.

* Corresponding author.
E-mail address: benjamin.lassagne@insa-toulouse.fr (B. Lassagne).

1631-0705/$ – see front matter
doi:10.1016/j.crhy.2010.06.006

1. Introduction

Nanoelectromechanical systems (NEMS) are very appealing devices. They have demonstrated ultrasensitive mass, force or magnetic sensing [1–4] and they can be used for radio frequency signal processing [5,6]. A NEMS also represents a model system to observe quantum behaviour in a macroscopic system [7–9]. The key parameters of NEMS which have enabled those applications are their high mechanical resonance frequency (in the microwave range), their low active mass (in the femtogram range) and their high quality factor (up to ten thousands). Up to now, the principal approach to fabricate NEMS was to use material such as silicon, silicon carbide or gallium arsenide and micro-fabrication techniques such as anisotropic plasma etching and electron beam lithography.

An alternative and very promising approach to build high performance NEMS could be to use carbon nanotubes (CNT) [10–18]. Indeed, they have exceptional mechanical properties, their cross section of the order of the nanometer enables the reduction of the active mass in the range of the atto-gram, their Young modulus reaches 1 TPa and their high structural quality and surface without dangling bonds are essential to obtain high quality factors. They also demonstrated remarkable electronic properties, such as ballistic electronic conduction [19], very regular Coulomb blockade regime [19] and they can serve to build high performance transistors [20].

We review in this article the method of fabrication of a CNT mechanical resonator and the electromechanical methods to actuate and detect its motion. Then we present experimental results demonstrating how the electromechanical coupling can be used to widely tune the CNT mechanical properties and to access the non-linear dynamics of the motion. Finally, we present one of the first demonstrations of the exceptional capabilities of CNT for mass sensing.

2. CNT fabrication

In the first step of the fabrication process, carbon nanotubes are grown by Chemical Vapour Deposition (CVD) of CH_4 at 900 °C directly on a highly doped silicon substrate coated with a 1 µm silicon oxide layer [21]. After the growth, the CNT are localized by atomic force microscopy (AFM) and connected with two Au/Cr (50/5 nm) contacts using electron beam lithography and metallic evaporation. The last step is the release of the CNT from the substrate by wet etching in a hydrofluoric acid buffer. At the end of the process, a thermal annealing is carried out at 400 °C during few hours in an Ar/H_2 environment in order to remove the contaminants leaving by the resist used for the metallic contact deposition step. Our typical devices have a length between contacts around 1 µm and have diameter around 1.2 nm.

3. Device actuation and detection

The CNTs are actuated by means of electrostatic interactions. By applying an oscillating voltage $V_g^{AC}\cos(2\pi ft)$ between the drain contact and the silicon backgate, the CNT undergoes an oscillating electrostatic force F_{elec} which reads

$$F_{elec} \approx \frac{1}{2}C_g' V_g^{DC^2} + C_g' V_g^{DC} V_g^{AC}\cos(2\pi ft) \tag{1}$$

with V_g^{DC}, the DC voltage and C_g' the derivative of the capacitance between the CNT and the backgate as a function of their distance.

To detect the mechanical motion, we use the CNT itself as a motion sensor. Indeed, the conductance G of the CNT depends on the electronic charge q_{CNT} inside the CNT. q_{CNT} is controlled by the gate capacitance C_g. Hence, when the CNT is oscillating, a charge variation δq_{CNT} is induced and reads $\delta q_{CNT} = V_g^{DC} C_g' \delta z$ with δz the mechanical motion amplitude; it induces in turn a modulation of G. To measure these high frequency conductance oscillations, we employ a mixing technique which consists to apply a second oscillating voltage between the source and the drain at a frequency $f + \delta f$ and amplitude V_{SD}. Then, the CNT acts as a mixer [11] and we measure with standard lock-in techniques the mixing current I_{mix} at the frequency δf which is fixed at a few kilohertz. I_{mix} can be written:

$$I_{mix} = \frac{1}{2}V_{SD}\frac{dG}{dV_g}\left(V_g^{AC}\cos(\alpha) + V_g^{DC}\frac{C_g'}{C_g}\delta z\cos(\alpha - \theta_m)\right) \tag{2}$$

with $\frac{dG}{dV_g}$ the CNT transconductance, α the electronic phase coming from the electronic circuitry and θ_m the phase between F_{elec} and the mechanical motion. The first term of Eq. (2) is purely electric and yields to a background current at any frequency, while the second term comes from the CNT mechanical motion. This last term has a non-negligible contribution when f matches the CNT mechanical resonance frequency f_0 which means that δz is maximal. Fig. 1c shows a typical CNT characteristic. I_{mix} is represented in colour as a function of V_g^{DC} and f. Superimposed to a background current (first term of Eq. (2)) we observe two lines which are the signature of the actuation of two different mechanical modes. We note that the V_g^{DC} dependence of f_0 comes from the static part of the force (first term of Eq. (1)) which bends the CNT and increases in turn its mechanical tension and then its mechanical resonance frequency.

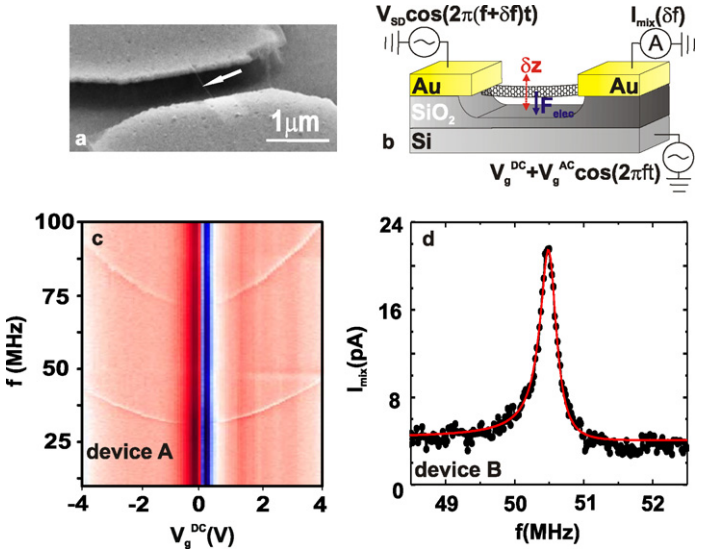

Fig. 1. (a) Scanning electronic microscope image of a typical CNT. The single wall carbon nanotube is pointed by a white arrow. (b) Schematic of a CNT resonator with the electrical connection on the gate and between the two gold contacts serving for the actuation and the detection of the mechanical motion. (c) Colour scale plot of I_{mix} as a function of V_g^{DC} and f at 300 K under a vacuum of 10^{-6} mbar and for $V_{SD} = V_g^{AC} = 25$ mV and $\delta f = 10$ kHz. (d) Measured mechanical resonance of a CNT as a function of f and for a fixed gate voltage. The red curve is a fit using Eq. (3). (For interpretation of the references to colour in this figure legend, the reader is referred to the web version of this article.)

For a small excitation V_g^{AC}, the CNT can be modelled with a harmonic oscillator characterized by its resonance frequency $2\pi f_0 = \sqrt{k/m_{eff}}$ with k, the stiffness constant of the nanotube and m_{eff} the effective mass. The motion amplitude as a function of f has a quasi-Lorentzian shape which reads

$$\delta z = \frac{1}{2\pi}\frac{F_{elec}}{m_{eff}}\frac{1}{\sqrt{(f^2 - f_0^2)^2 + (f f_0/Q)^2}} \tag{3}$$

Q is the quality factor quantifying the mechanical energy dissipation. Hence from the mixing current we can extract easily the fundamental characteristics of our resonators, f_0 and Q. Our devices have frequency ranging from 20 MHz to 200 MHz between 300 K and 4 K and have Q ranging from 100–200 at 300 K up to 2000 at 4 K.

4. Influence of the electromechanical coupling on the mechanical properties of the CNT at low temperature

The coupling between the electronic charge motion and the mechanical motion is a fundamental parameter for an electromechanical resonator as it allows us to actuate and detect the mechanical motion. To be able to quantify its strength and understand its influence on the mechanical properties is fundamental both for technological applications and fundamental issue in physics.

To investigate the coupling between mechanic and charge motion in CNT, we have carried out electromechanical measurements at low temperatures on a single wall CNT fabricated as described in Section 2 and by using the mixing technique described above [17]. Fig. 2a shows the differential conductance dI/dV as a function of V_g^{DC} and V_{SD}. The regular diamond shape of dI/dV is typical of a Coulomb blockade regime. It means that the device behaves as a single dot between the two contacts; its charge q_{dot} is quantized and can be controlled one by one by V_g^{DC} as we can observe on Fig. 2c. As a consequence of this peculiar behaviour of q_{dot}, the zero bias voltage differential conductance G oscillates as a function of V_g^{DC}. G is maximum for V_g^{DC} where q_{dot} can be increased or decreased by one and G equals to zero (at $T = 0$ K) when q_{dot} is constant (Fig. 2d). Fig. 2b shows a colour plot of the mixing current as a function of V_g^{DC} and f at 4 K. We can extract from I_{mix} the parameters Q and f_0. They show a very interesting behaviour as a function of V_g^{DC}, they oscillate with the same period, the same phase as the experimental G as we can see on Figs. 2e, 2f and 2g. When G is maximal Q and f_0 are minimal.

This striking behaviour is a direct consequence of the peculiar dependence of q_{dot} on V_g^{DC}. As explained in Section 2, when the nanotube oscillates, the gate capacitance oscillates and, in turn, q_{dot} oscillates. However, as the nanotube is in the Coulomb blockade regime the oscillation amplitude of the charge δq_{dot} will have a non-trivial dependence on V_g^{DC}, as we can see on Fig. 2c (green trace and blue trace); δq_{dot} follows the V_g^{DC} dependence of G, it is maximum (minimum) when G is maximum (minimum). This coupling between the mechanical motion and the charge motion directly affects the

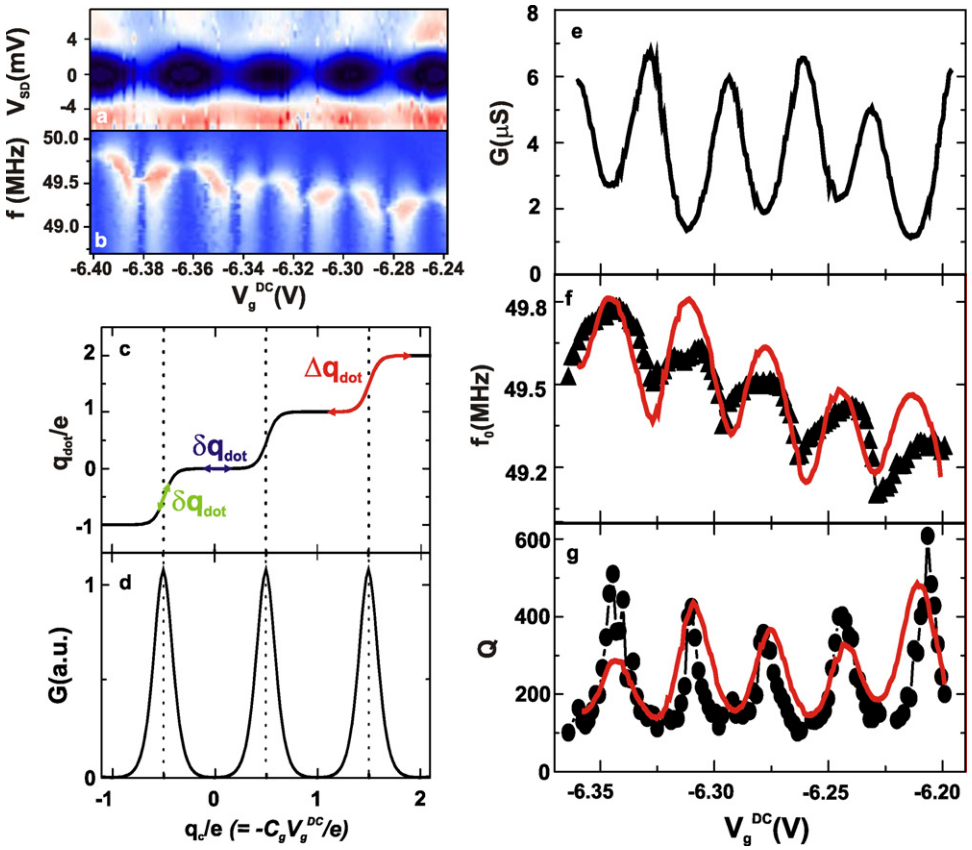

Fig. 2. (a) Colour plot of the differential conductance of the device as a function of the V_g^{DC} and V_{SD} at 4 K. Blue colour and red colour correspond respectively to low and high conductance. The shape is consistent with a Coulomb blockade regime. (b) Colour plot of the mixing current as a function of f and V_g^{DC} at 4 K. Blue colour corresponds to low current and red colour to high current. The red lobes traduce the actuation of the CNT. (c), (d) Electronic charge q_{dot} and zero bias differential conductance $\boldsymbol{G}$ of the device as a function of V_g^{DC} in the Coulomb blockade regime. The green and blue traces represent the amplitude of the charge motion δq_{dot} when the nanotube oscillates in the linear regime. When G is maximum (minimum) the δq_{dot} amplitude is maximum (minimum). The red trace represents the charge motion when the nanotube oscillates with higher amplitude; it is driven in a non-linear regime. (e), (f), (g) Experimental zero bias voltage differential conductance, mechanical resonance frequency (black curve) and quality factor (black curve) of the device at 4 K. The entire characteristics have the same period and the same phase. The red curves represents the fit with Eq. (5). We obtained a rather good agreements between experiments and theory.

electrostatic force undergone by the CNT. Indeed, in the Coulomb blockade regime the mechanical motion induces variation of the electrostatic force which reads [17]

$$\delta F_{elec} = E_c \left(\frac{C_g' V_g^{DC}}{e} \right)^2 \left(\frac{\mathrm{d}q_{dot}}{\mathrm{d}V_g^{DC}} - 1 \right) \delta z \tag{4}$$

with E_c the charging energy of the nanotube. The amplitude of oscillation of the electrostatic force takes different amplitude as a function of V_g^{DC}, is maximum (minimum) when the slope $\frac{\mathrm{d}q_{dot}}{\mathrm{d}V_g^{DC}}$ is maximum (minimum). We also need to consider the dynamic of the charge motion, δq_{dot} does not answer instantaneously to the mechanical motion because of the finite tunnelling rate Γ of the barriers at the contacts. A simple classical picture allowing us to capture the motion's dynamic effect is to consider that the charge motion answer with a time $\tau \sim 1/\Gamma$ to the mechanical motion [22]. Hence

$$\delta F_{elec}(t) \propto \delta z(t-\tau) \propto \delta z(t) - \tau \delta \dot{z}(t)$$

The first term of this expression is proportional to the mechanical motion and hence equivalent to a spring force. It causes a tuning of the CNT spring constant and thus a tuning of its mechanical resonance frequency. Concerning the second term of this equation, it is proportional to the derivative of the motion, and then it is equivalent to a damping force. It is responsible of the quality factor oscillation. To describe properly the charge motion we use the framework of a master equation approach. We can show that the quality factor and the oscillation amplitude of the frequency are given by, [17]:

$$\frac{1}{Q} = 2\pi f_0 \frac{(C_g' V_g^{DC})^2}{k} \left(\frac{2E_c}{e^2 \Gamma} \right)^2 G$$

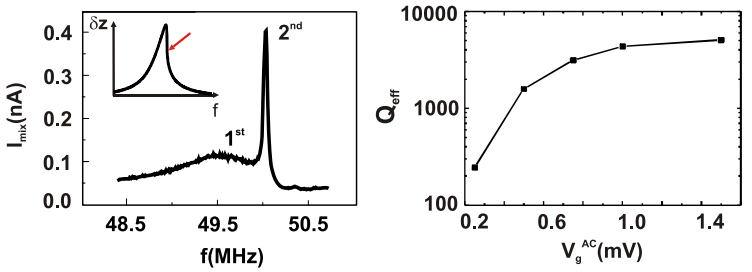

Fig. 3. (a) Mixing current as a function of f at 1.5 K in the non-linear regime. The second peak has a quality factor as high as 5100. Insert: shark fin shape of the motion δz as a function of f when the resonator behaves as a Duffing oscillator. (b) Quality factor of the narrow peak as a function of the driving voltage V_g^{AC} at 1.5 K.

$$\delta f_0 = -\frac{f_0}{2}\frac{(C_g' V_g^{DC})^2}{k}\frac{E_c}{e^2}\left(\frac{2E_c}{e^2\Gamma}G - 1\right) \tag{5}$$

To compare this model with experiment we take as fitting parameter C_g'/k and Γ. Figs. 2f and 2g show that this model reproduces with a rather good agreement our experimental data. Moreover we obtained values for the fitting parameters in a good agreement with theory.[1] There results show that the main dissipation mechanism at low temperature comes from the coupling between mechanics and charge transport.

We now look at measurements where the excitation voltage allows driving the CNT into a non-linear regime. Fig. 3 shows the mixing current of the device in these experimental conditions. We observe a very surprising phenomenon: the peak in the mixing current induced by the actuation of the CNT splits in two peaks, a broad one and a narrow one (Fig. 3a). The narrow peak appears only close to a conductance peak. The most striking behaviour is that the quality factor of the narrow peak increases when the excitation voltage increases, it can reach a value as high as 5100 which is 50 times higher than the quality factor of the broad peak. The coupling between the mechanic and the charge motion in the CNT is at the origin of this behaviour. Indeed, at a higher excitation voltage, the CNT mechanical motion enters into a non-linear regime which is well described by a Duffing oscillator [25] in which δz as a function of f has not a quasi-Lorentzian shape, but has a shark fin shape which is characteristic of mechanical non-linearity. Concerning the electronic properties, because of the stepwise dependence of q_{dot} as a function of V_g^{DC}, the higher amplitude of the motion induces a non-trivial behaviour of the charge motion as we can observe on Fig. 2c (Δq_{dot} red trace). The splitting of the peak is a direct consequence of this non-trivial behaviour of the electronic properties while the asymmetry between the broad peak and the narrow peak comes from the shark fin shape and especially because of the sharp decrease of the motion amplitude just after the resonance frequency (pointed by an arrow on the insert of Fig. 3a). This surprising phenomenon could be very useful to increase the sensitivity of CNT for mass or force sensing which rely on precise frequency measurements. Indeed, the smallest frequency shift detectable is proportional to the inverse square root of the quality factor; it means that by measuring the frequency with the narrow peak we could sensibly increase the sensitivity of the device.

These experimental results have shown that the mechanical coupling is very strong in the carbon nanotube and allow us to widely tune the mechanical properties and to access the non-linear dynamic of the motion. In comparison, experiments made by coupling a silicon beam with a metallic single electron transistor do not yield such tuning of the mechanical properties [7]. The major reason is that carbon is lighter than a silicon beam and therefore is more sensitive to the force induced by one electron.

5. Ultrasensitive mass sensing with a CNTER

The use of NEMS for mass sensing is very promising [26]. Indeed, it should open new opportunities for ultrasensitive mass spectroscopy, for instance to weigh an individual protein, molecule or even a single atom. A lot of efforts has been made these last two decades to increase the mass resolution of NEMS. It has been increased by 12 orders of magnitude, from few 10^{-9} g in 1993 [27] to 7×10^{-21} g (zg) in 2006 [1]. This huge increase has been possible by shrinking the mechanical resonators using top down micro/nano-fabrication techniques. However, it becomes very difficult using micro-fabrication techniques to reach few nanometers. The alternative approach to micro-fabrication would be to use materials grown chemically and having nano-dimensions like carbon nanotubes. Indeed, they have a very small diameter of the order of 1 nm which is not attainable using micro/nano-fabrication techniques.

[1] We obtain $C_g'^2/k = 6 \times 10^{-22}$ F^2/Nm, which has to be compared to $C_g' \approx 10^{-13}$–10^{-12} F/m obtained using commercial simulators and $k \approx 10^{-4}$–10^{-3} N/m from [11]. The value of Γ is $3 \cdot 10^9$ s^{-1}, which is somewhat smaller than expected in the quantum regime $\Gamma = 8k_B T G_{\max}/e^2 \approx 9 \times 10^{10}$ s^{-1} (with $G_{\max}$ the maximum conductance of a Coulomb blockade peak). In addition, the shape of the measured oscillations of f_0 and Q differs to some extent from what is predicted (Fig. 2d). These differences may arise from the fact that the nanotube dot is not perfect (the Coulomb blockade peaks are not fully periodic in V_g^{DC} and the peak heights are different). Another explanation is that the model used is too simple to quantitatively capture the physics [23,24].

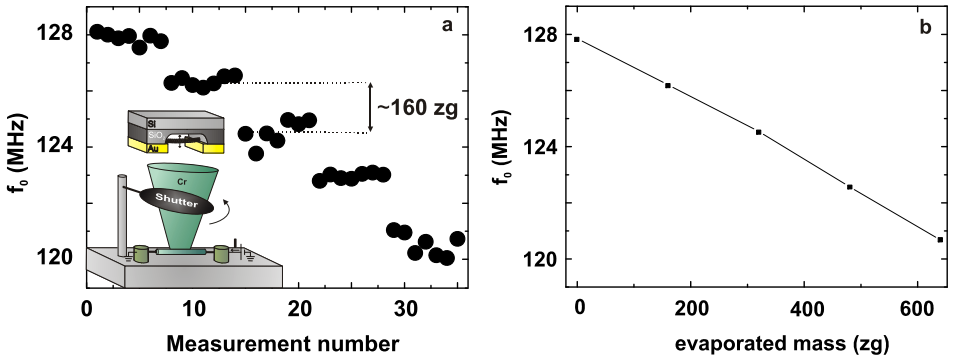

Fig. 4. (a) Resonance frequency of the device measured sequentially. f_0 is shifted each time 160 zg of Cr is evaporated. f_0 is determined by measuring the mixing current of the device as a function of the actuation frequency. A frequency point is recorded each 40 s except when Cr is evaporated, we wait 5 min before measuring f_0. The insert represents a schematic of the mass sensing experiment. The device is installed in a Joule heating metal evaporation system where Cr is evaporated by passing a current of few amps in a Cr bar. The shutter is used to block the Cr flow arriving onto the carbon nanotube. The experiment is performed at 300 K under 10^{-6} mbar. (b) Frequency as a function of the evaporated mass. The slope 11 $\mathrm{Hz}\cdot\mathrm{yg}^{-1}$ gives the responsitivity of the device.

Even though the mass sensing experiment with a mechanical resonator is very challenging, the principle remains simple. The mechanical resonance frequency f_0 depends on the resonator total mass; hence by depositing the species to weigh on the resonator, we can tune f_0. The frequency shift δf induced by the change of mass δm reads:

$$\delta f \approx \frac{f_0}{2m_{eff}}\delta m \tag{6}$$

where $\frac{f_0}{2m_{eff}}$ defines the responsitivity $\Re$ of the mass sensor. It is an important parameter used to evaluate the resonator performances. The higher $\Re$, the better the resonator is for mass sensing.

To determine the capabilities of our CNT for mass sensing, we installed them in a Joule heating metal evaporation system in order to depose under vacuum (10^{-6} mbar) and in a control way Cr atoms onto the surface of the CNT [15] (insert Fig. 4a). We choose Cr because of its high binding energy on the CNT surface [28]. The experiment is carried out as following: first, we measure several times the resonance frequency of the CNT to control the frequency stability, and then we evaporate Cr atoms during 1.5 s. We repeat this sequence several times. Fig. 4a shows the resonance frequency of a typical resonator for different Cr evaporation sequences. We observe each time Cr atoms are evaporated a very reproducible frequency shift. It corresponds to 160 zg of Cr atoms deposited onto the CNT. This mass is calculated by considering the exposed area of the nanotube (which equals to its length L times its radius r) and the evaporation rate of the Joule heating evaporation system. This last parameter was precisely measured thanks to a reference sample where Cr is evaporated during 120 s in the same experimental condition than the mass sensing experiment. On the reference sample a square structure was patterned in PMMA (polymethyl methacrylate). Then, the thickness of the Cr structure was measured by AFM in order to estimate precisely the evaporation rate. We found roughly 10 $\mathrm{pm\,s}^{-1}$.

Fig. 4b shows the frequency as a function of the evaporated mass. The slope corresponds to the responsitivity of the CNT. We found an exceptional $\Re$ of the order of 11 $\mathrm{Hz}\cdot\mathrm{yg}^{-1}$. It surpasses by a factor 10 000 the responsitivity of the best silicon carbide micro-fabricated beam [1]. Having estimated $\Re$ we can determine the mass resolution (the smallest mass detectable) of our device by measuring the noise frequency δf given by $\delta f = \sqrt{\langle (f - \langle f \rangle)^2 \rangle}$. For our device δf is likely limited by the fluctuations of the electric readout circuitry. We measure at 300 K a δf of the order of 280 kHz and at 4 K δf roughly equals to 15 kHz. It corresponds to a mass resolution of 25 zg and 1.7 zg respectively. Again, it has to be compared to the resolution of the best micro-fabricated beam which is around 7 zg at 4 K.

Two other groups reported very similar results [14,16]. Hence, carbon nanotubes are currently the most sensitive nanobalance made so far. This capability is a direct consequence of the very small mass of CNT. However, we have to emphasize that even though $\Re$ is four orders of magnitude better than for a silicon material based mechanical resonator, the mass resolution is only four times better. This huge difference comes from the fact much efforts have been made for many years to optimize micro-fabricated beams. Hence the frequency noise has been decreased to the thermo-mechanical limit [1] which has not already been reached for carbon nanotubes. Future work will be focused on the improvement of the frequency noise of CNT in order to reach the thermo-mechanical limit which should allow us to access a mass resolution in the range of 1 yg, the mass of one neutron [15].

6. Conclusion

These experimental results have shown that carbon nanotubes are a material of choice to build a versatile nanomechanical resonator. First, the strong electromechanical coupling between the mechanic and the charge motion ease the detection of the mechanical motion at the nanoscale and enable to widely tune the mechanical properties and the non-linearity in

carbon nanotubes. It hold promise for various applications in quantum measurements and quantum manipulation [29,30], for ultrasensitive sensing [31], mechanical signal amplification [32,33] or mechanical microwave computing [34]. Second, in parallel with two other groups we have shown that carbon nanotubes, without device optimization, are the most sensitive nanobalance made so far. It let us envisage for the future how will be sensitive a carbon nanotube for different kind of sensing: (i) mass, the maximum sensitivity expected is of the order of 1 yg; (ii) force, we expect to go under 10^{-18} N; and (iii) magnetic sensing, where carbon nanotubes could allow us to study single magnetic nano-object having magnetization around few Bohr magneton [35].

References

[1] Y.T. Yang, C. Callegari, X.L. Feng, K.L. Ekinci, M.L. Roukes, Nanolett. 6 (2006) 583.
[2] H.J. Mamina, D. Rugar, Appl. Phys. Lett. 79 (2001) 3358.
[3] D. Rugar, R. Budakian, H.J. Mamin, B.W. Chui, Nature 430 (2004) 329.
[4] M. Li, H.X. Tang, M.L. Roukes, Nat. Nanotechnol. 2 (2007) 114–120.
[5] C.T.C. Nguyen, IEEE Trans. Microwave Theory Tech. 47 (1999) 1486–1503.
[6] C.T.C. Nguyen, A.-C. Wong, D. Hao, in: Solid-State Circuits Conf., 1999, pp. 78–79.
[7] R.K. Knobel, A.N. Cleland, Nature 424 (2003) 291.
[8] M.D. LaHaye, O. Buu, B. Camarota, K.C. Schwab, Science 304 (2004) 74.
[9] A. Naik, O. Buu, M.D. LaHaye, A.D. Armour, A.A. Clerk, M.P. Blencowe, K.C. Schwab, Nature 443 (2006) 193.
[10] P. Poncharal, Z.L. Wang, D. Ugarte, W.A. Heer, Science 283 (1999) 1513.
[11] V. Sazonova, Y. Yaish, H. Üstünel, D. Roundy, T.A. Arias, P.L. McEuen, Nature 431 (2004) 284.
[12] B. Witkamp, M. Poot, H.S.J. van der Zant, Nanolett. 6 (2006) 2904.
[13] D. Garcia-Sanchez, A. San Paulo, M.J. Esplandiu, F. Perez-Murano, L. Forró, A. Aguasca, A. Bachtold, Phys. Rev. Lett. 99 (2007) 085501.
[14] K. Jensen, K. Kim, A. Zettl, Nature Nanotech. 3 (2008) 533.
[15] B. Lassagne, D. Garcia-Sanchez, A. Aguasca, A. Bachtold, Nanolett. 8 (2008) 3735.
[16] H.-Y. Chiu, P. Hung, H.W.C. Postma, M. Bockrath, Nanolett. 8 (2008) 4342.
[17] B. Lassagne, Y. Tarakanov, J. Kinaret, D. Garcia-Sanchez, A. Bachtold, Science 325 (2009) 1107.
[18] G.A. Steele, A.K. Hüttel, B. Witkamp, M. Poot, H.B. Meerwaldt, L.P. Kouwenhoven, H.S.J. van der Zant, Science 325 (2009) 1103.
[19] J.-C. Charlier, X. Blase, S. Roche, Rev. Mod. Phys. 79 (2007) 677.
[20] M.P. Anantram, F. Leonard, Rep. Prog. Phys. 69 (2006) 507–561.
[21] J. Kong, H.T. Soh, A.M. Cassell, C.F. Quate, H. Dai, Nature 395 (1998) 878.
[22] A. Clerk, S. Bennett, New J. Phys. 7 (2005) 238.
[23] A.D. Armour, M.P. Blencowe, Y. Zhang, Phys. Rev. B 69 (2004) 125313.
[24] F. Pistolesi, S. Labarthe, Phys. Rev. B 76 (2007) 165317.
[25] L.D. Landau, E.M. Lifshitz, Mechanics, Pergamon Press, 1960.
[26] A.K. Naik, M.S. Hanay, W.K. Hiebert, X.L. Feng, M.L. Roukes, Nat. Nano. 4 (2009) 445–450.
[27] J.P. Cleveland, S. Manne, D. Bocek, P.K. Hansma, Rev. Sci. Instrum. 64 (1993) 403.
[28] Y. Zhang, F.W. Nathan, R.J. Chen, H. Dai, Chem. Phys. Lett. 331 (2000) 35.
[29] V. Peano, M. Thorwart, Phys. Rev. B 70 (2004) 235401.
[30] S. Zippilli, G. Morigi, A. Bachtold, Phys. Rev. Lett. 102 (2009) 096804.
[31] J.S. Aldridge, A.N. Cleland, Phys. Rev. Lett. 94 (2005) 156403.
[32] A. Erbe, et al., Appl. Phys. Lett. 77 (2000) 3102.
[33] R.L. Badzey, P. Mohanty, Nature 437 (2005) 995.
[34] S.B. Shim, M. Imboden, P. Mohanty, Science 316 (2007) 95.
[35] B. Lassagne, M. Respaud, in preparation.